Vol. 07, No. SI♣, pp. 30 –36 (2026)
ISSN: 2708-0757

JOURNAL OF APPLIED SCIENCE AND TECHNOLOGY TRENDS

www.jastt.org

Quantitative Evaluation of Adaptive Threshold-Based Denoising for AWGN-Corrupted Images Using Multiresolution Discrete and Stationary Wavelet Transforms

Firas Mahmood Mustafa[1,*], Jalal Sami Issa[2,3]

[1]*Cybersecurity Eng., Dept., Technical College of Engineering, Duhok Polytechnic University, Kurdistan Region of Iraq, firas.mahmoud@dpu.edu.krd*
[2]*Information Technology Dept., Technical College of Duhok, Duhok Polytechnic University, Kurdistan Region of Iraq jalal.sami@dpu.edu.krd*
[3]*Information Technology Dept., Technical College of Informatics, Akre University for Applied Sciences, Kurdistan Region of Iraq, jalal.sami@auas.edu.krd*

**Correspondence: firas.mahmoud@dpu.edu.krd*

Abstract

The integrity of digital images is often degraded by Additive White Gaussian Noise (AWGN), necessitating efficient denoising solutions. This study presents a comprehensive, quantitative benchmark of wavelet-based denoising by systematically evaluating the synergy between transform types and thresholding strategies. The main contributions of this work are threefold. First, it conducts a large-scale comparative analysis of 117 wavelet filters across both the Discrete Wavelet Transform (DWT) and the Stationary Wavelet Transform (SWT). Second, it integrates these transforms with both hard and adaptive SURE Shrink soft thresholding, evaluating their performance under two AWGN levels (σ=15, σ=25) on standard test images using Peak Signal-to-Noise Ratio (PSNR), while acknowledging the importance of perceptual metrics such as SSIM for future evaluation. Third, the results establish that SWT consistently yields higher PSNR than DWT, and SURE Shrink outperforms hard thresholding. Their combination achieved the best results, with average PSNR improvements of 15.26% and 13.23% over DWT for low and high noise, respectively. While the study is limited by its use of a single metric and grayscale images, the findings position SWT paired with SURE Shrink soft thresholding as a promising and competitive approach for image restoration in the presence of AWGN. Additionally, the study is primarily experimental, and further theoretical modeling is identified as future work.

Keywords: *Image Denoising, AWGN, Wavelet Transform, DWT, SWT, SURE Shrink, PSNR.*
Received: October 04th, 2025 /Revised: March 15th, 2026 / Accepted: April 13th, 2026 / Online: April 19th, 2026

I. INTRODUCTION

In fields such as medical diagnostics, remote sensing, and multimedia, the critical importance of digital image quality is widely recognized. A principal challenge to this quality is posed by Additive White Gaussian Noise (AWGN), a common artifact that is introduced during image acquisition and transmission, thereby degrading visual clarity and compromising analytical value [1, 2]. The development of effective denoising strategies has thus long been regarded as a cornerstone of image processing research. Traditional approaches, including spatial filters, have been found to often sacrifice edge detail for noise reduction [3]. This limitation prompted a shift towards multiscale transform-domain methods, with wavelet-based techniques being established as a powerful paradigm due to their ability to localize signal and noise in distinct coefficients [4]. Among these, the Discrete Wavelet Transform (DWT) and the Stationary Wavelet Transform (SWT) are considered two foundational pillars. While DWT is valued for its compact representation, it is also known to be susceptible to shift-variance, which can lead to artifacts.

In contrast, SWT is characterized by its shift-invariance, which is achieved by forgoing downsampling, and is generally

doi: 10.38094/jastt7031085

associated with superior structural preservation, making it particularly well-suited for denoising tasks [5, 6]. This fundamental difference between DWT and SWT plays a critical role in denoising performance. The shift-variance property of DWT may result in instability in coefficient representation under small signal variations, whereas the shift-invariance of SWT ensures more consistent coefficient alignment across scales. Consequently, SWT is often more effective in preserving edges and fine structures, particularly in applications where spatial fidelity is essential.

The efficacy of these transforms is heavily influenced by the thresholding function applied to wavelet coefficients. Here, simple hard thresholding is often outperformed by adaptive soft thresholding methods like SURE Shrink, in which optimal thresholds are data-adaptively determined using Stein's Unbiased Risk Estimate, thereby achieving a better balance between noise removal and detail retention [7, 8].

More recently, the field has been transformed by deep learning. Remarkable performance has been demonstrated by models such as DnCNN, FFDNet, and SwinIR, which learn noise characteristics from vast datasets [9, 10]. Despite their superior performance, a direct comparison with deep learning-based methods is beyond the scope of this study, as such approaches require extensive training datasets, parameter tuning, and computational resources. In contrast, this work focuses on classical, training-free methods to provide a fair and reproducible benchmark under controlled conditions. However, their practical deployment is often constrained by substantial computational demands, a reliance on extensive training data, and an inherent lack of interpretability.

In contrast, SWT is recognized as a transparent, model-based alternative that requires no training and provides robust, interpretable results with comparatively low computational cost, thereby sustaining its relevance. Despite the maturity of wavelet denoising, a significant gap is identified in the comprehensive, large-scale benchmarking of DWT and SWT under consistent conditions, particularly when integrated with adaptive thresholding across a wide array of wavelet families. Many previous studies have been limited to a handful of filters, leaving the question of the optimal wavelet-thresholding combination inadequately addressed. This gap is addressed in the present study through an exhaustive comparative analysis. The novelty of this work is defined by the systematic evaluation of 117 distinct wavelet filters within both DWT and SWT frameworks, which are combined with hard and SURE Shrink thresholding to denoise standard images corrupted by AWGN at two noise levels.

Performance is quantitatively assessed primarily using the Peak Signal-to-Noise Ratio (PSNR), a widely accepted fidelity metric [11], to provide a clear and reproducible benchmark. While PSNR is employed as the primary quantitative evaluation metric due to its simplicity, reproducibility, and widespread use in benchmarking studies, it is acknowledged that PSNR does not always correlate well with human visual perception. Therefore, incorporating perceptual quality metrics such as SSIM, MSSIM, and FSIM would provide a more comprehensive evaluation of visual quality.

Furthermore, it is acknowledged that the current study primarily emphasizes experimental evaluation. The development of a formal mathematical model and analytical framework to theoretically characterize the behavior of wavelet-based adaptive thresholding methods is an important direction that will be addressed in future work [10].

The primary contribution of this research is therefore the establishment of a definitive, large-scale reference for the selection of optimal wavelet-based denoising configurations, offering practical guidance for applications where computational efficiency, interpretability, and reliable performance are deemed paramount.

II. Research Objectives

This study aims to quantitatively evaluate the performance of adaptive thresholding-based image denoising algorithms using multiresolution wavelet transforms. The core objectives include:

1) *Comparing the denoising effectiveness of Discrete Wavelet Transform (DWT) and Stationary Wavelet Transform (SWT) frameworks.*
2) *Assessing the impact of different thresholding methods, specifically Hard and SURE Shrink thresholding, on denoising outcomes.*
3) *Measuring and analyzing denoising quality using PSNR as a quantitative metric under various noise levels ($\sigma = 15$ and $\sigma = 25$).*
4) *Evaluating the computational complexity of the proposed DWT and SWT denoising frameworks to assess their practical feasibility.*
5) *Determining the optimal wavelet families and filters for image restoration under additive white Gaussian noise (AWGN) based on a composite criterion of PSNR and edge preservation.*

III. Novelty and Contribution

The novelty of this research lies in its comprehensive comparative analysis of 117 wavelet filters across both DWT and SWT domains using adaptive thresholding techniques. While the core decomposition was performed using the commonly adopted Daubechies (db4) wavelet as a baseline, the experimental framework was uniquely extended to benchmark this broad spectrum of 117 filters under standardized noise conditions. Unlike previous studies that often focus on limited wavelet families or fixed thresholding strategies, this work provides an extensive empirical evaluation.

Furthermore, the inclusion of a PSNR-based quantitative framework across multiple images ensures a reproducible and robust assessment. This research serves as a valuable reference for selecting optimal wavelet-thresholding combinations in practical denoising applications.

IV. Literature Review

Image denoising remains a central task in digital image processing, as random noise-particularly Additive White Gaussian Noise (AWGN)—frequently corrupts images during

acquisition or transmission, degrading visual quality and structural details [15], [16]. Early denoising methods, including linear and nonlinear spatial filters, provided basic noise suppression but often compromised edge fidelity [17]. These limitations spurred the adoption of transform-domain approaches, notably wavelet-based techniques, which offer multiscale analysis and better separation between signal and noise [18].

Among wavelet frameworks, the Discrete Wavelet Transform (DWT) provides an efficient, non-redundant representation but suffers from shift-variance, which can lead to artifacts in the denoised image. In contrast, the Stationary Wavelet Transform (SWT) maintains translational invariance at the cost of redundancy, which significantly enhances edge preservation and structural consistency [19], [20]. Within these wavelet domains, thresholding techniques serve as the core mechanism for noise suppression. Hard thresholding removes small coefficients entirely, offering a straightforward approach, while soft thresholding—especially the adaptive SURE Shrink method-attenuates them based on statistical criteria to reduce artifacts and produce smoother visual results [21], [22].

In recent years, the field has been revolutionized by modern deep learning paradigms. Convolutional Neural Networks (CNNs) have demonstrated remarkable success by learning complex noise patterns from vast datasets, while Generative Adversarial Networks (GANs) have been explored for generating highly realistic, clean images from noisy inputs. More recently, Transformer-based models, with their powerful self-attention mechanisms, have shown great promise in capturing long-range dependencies in images for superior denoising. Despite their impressive performance, these data-driven methods often require substantial computational resources and large, annotated training datasets, which can limit their applicability in scenarios where data is scarce or interpretability is key [6], [9]. This has encouraged a parallel interest in hybrid methods that seek to combine the interpretability and mathematical foundation of traditional techniques with the power of modern learning. For instance, several studies have begun integrating wavelet transforms with non-local means filtering or using CNNs to learn optimal parameters within a wavelet-based denoising pipeline, aiming to harness the strengths of both worlds [4,10].

Although many studies have demonstrated the individual benefits of DWT, SWT, and various thresholding techniques, a comprehensive and systematic comparison under consistent conditions has been less common. Many prior works have compared only a limited selection of wavelet filters or have not evaluated performance across multiple, standardized noise levels. This study directly addresses this gap by conducting an extensive evaluation of 117 distinct wavelet filters across both DWT and SWT domains, combined with hard and soft thresholding, under two well-defined noise intensities. By assessing denoising performance using PSNR across this broad experimental framework, our work provides deeper, more generalizable insights into the relative strengths of these classical yet powerful techniques in restoring AWGN-corrupted images.

V. METHODOLOGY

A. Overview

This study aims to quantitatively evaluate the performance of wavelet-based denoising techniques applied to images corrupted with Additive White Gaussian Noise (AWGN). Two wavelet frameworks—Discrete Wavelet Transform (DWT) and Stationary Wavelet Transform (SWT)—are compared using two thresholding strategies: hard thresholding and the adaptive SURE Shrink soft thresholding. The evaluation is based on Peak Signal-to-Noise Ratio (PSNR), a standard metric for image quality assessment.

B. Test Images and Noise Simulation

Lena, Butterfly, and Cameraman were selected as standard benchmarks, widely used in denoising studies for their mix of textures, edges, and smooth regions. The inclusion of 117 filters across all wavelet families ensured that the evaluation captured the full diversity of wavelet characteristics, from compactly supported to highly symmetric filters. It should be noted that the use of grayscale benchmark images allows for controlled and consistent evaluation of denoising performance. However, this may limit the generalization of the results to more complex real-world scenarios, such as color images or domain-specific datasets.

C. Wavelet Decomposition

By expanding the scope of analysis, the experiments were expanded to include 117 waveform filters covering all families (Daubechies, Symlets, Coiflets, Biorthogonal, and Reverse Biorthogonal). This ensured a comprehensive benchmark of transform performance.

D. Thresholding Techniques

Two thresholding methods are applied to the high-frequency subbands [23]:

- *Hard Thresholding:* Coefficients below a fixed threshold are set to zero, preserving strong edges but potentially introducing artifacts. Threshold value is computed by applying the equation 1 as follows:

$$\boldsymbol{Th} = \frac{\boldsymbol{\sigma^2}}{\boldsymbol{\sigma_x}} \quad (1)$$

Where $\boldsymbol{\sigma_x}$ is the standard deviation (STD) of the sub-bands. σ^2 is the noise value of noisy image, which is computed by using Robust Median Estimator estimated from the sub-band HH by equation 2 below:

$$\sigma^2 = [\text{median}(|x(i,j)|)/0.6745]^2 \quad (2)$$

- *SURE Shrink (Soft Thresholding*): A data-driven method that adapts the threshold value per subband using Stein's Unbiased Risk Estimate (SURE), balancing denoising and detail retention. The adaptive nature of SURE-Shrink allows it to dynamically adjust threshold values according to the statistical distribution of wavelet coefficients within each subband. This

adaptability provides a more balanced compromise between noise suppression and detail preservation compared to fixed thresholding techniques, thereby improving overall denoising stability. Threshold value is computed by applying the steps as equation 3 to equation 10 below:

$$T\_univ = \hat{\sigma} \cdot \sqrt{2 \cdot ln(n)} \quad (3)$$

Where:

T_univ: VisuShrink (universal) threshold used as an upper cap.

n: number of coefficients in the current subband.

ln: natural logarithm; √(2 ln n) is inside the square root.

$$z_i = \frac{d_i}{\hat{\sigma}} \quad (4)$$

Where:

z_i: normalized coefficients with unit noise variance.

d_i: original (noisy) detail coefficients.

$\hat{\sigma}$: noise standard deviation from equation 1.

$$y_i = z_i^2, \quad y_{(1)} \leq y_{(2)} \leq \ldots \leq y_{(n)} \quad (5)$$

Where:

y_i: squared normalized coefficients.

$y_{(k)}$: k-th smallest value after sorting ascending.

$$SURE(t) = n - 2k + \Sigma\ (i = 1 \rightarrow)\ y_{(i)} + (n - k)t^2 \quad (6)$$

Where:

SURE(t): unbiased estimate of mean squared error for soft-threshold t (in normalized units).

n: number of coefficients.

k: count of coefficients with $y_i \leq t^2$ (equivalently $|z_i| \leq t$).

Σ (i=1→k) $y_{(i)}$: sum of the k smallest squared coefficients.

$(n - k)\ t^2$: penalty for coefficients shrunk by t above the threshold.

$$t* = arg\ min\_t\ SURE(t) \quad (7)$$

Where:

t*: threshold that minimizes SURE(t) over candidate values t (computed from the sorted $|z_i|$).

$$\tau* = \hat{\sigma} \cdot t* \quad (8)$$

Where:

τ*: SURE-Shrink threshold in the same units as d_i.

$\hat{\sigma}$: noise standard deviation.

t*: optimal normalized threshold (from eq. 7).

$$\tau_{SURE} = min(\tau*, \quad T_{univ}) \quad (9)$$

Where: τ_SURE: practical threshold used in denoising (often min of SURE and universal thresholds).

$$\hat{d}_i = sign(d_i) \cdot max(|d_i| - \tau_{SURE}, 0) \quad (10)$$

Where:

$\hat{d}_i$: thresholded coefficient.

sign(·): sign function (+1 for positive, −1 for negative, 0 at zero).

max(a, b): returns the larger of a and b.

τ_SURE: final threshold from Step 8 (or τ* if uncapped).

The low-frequency approximation band is left unaltered in all cases.

E. Inverse Reconstruction

After thresholding, inverse DWT and SWT are applied to reconstruct the denoised images. This step combines the preserved low-frequency band with the modified high-frequency coefficients to restore image structure.

F. Evaluation Metric

The quality of the denoised images is assessed using PSNR, where Higher PSNR values indicate better image quality. The PSNR can be defined as [24], [25], [26]:

$$\boldsymbol{PSNR = 10.log_{10}(\frac{MAX^2}{MSE})} \quad (11)$$

Where:

MAX is the maximum possible pixel value (255 for 8-bit images).

MSE is the Mean Squared Error between the original and denoised image, and it can be computed as below:

$$\boldsymbol{MSE = \left(\frac{1}{M.N}\right).\sum_{x=1}^{M}\sum_{y=1}^{N}[g(x,y) - f(x,y)]^2} \quad (12)$$

Where:

M is the quantity of rows in the input image.

N is the quantity of columns in the input image.

g is an input image (noise picture).

f is an output image (denoising picture).

Although PSNR is widely adopted for quantitative evaluation, it primarily measures pixel-wise differences and may not fully capture perceptual image quality. The inclusion of perceptual metrics such as SSIM or FSIM could provide additional insight into structural and visual fidelity; however, this is considered beyond the scope of the current study and is reserved for future work.

G. Experimental Setup

All experiments are implemented in MATLAB R2023a, and results are averaged over multiple runs to ensure robustness. In this work, three grayscale images each of size 256 × 256 are shown below in Figure 1 have been used as tested images. The noise type used is the Additive White Gaussian Noise (AWGN) with zero mean, and the values of the noise ratio used were σ =15, and σ =25. The AWGN noise is added to an image to create the noisy image.

For each noise level, every combination of wavelet transforms and thresholding method is tested on all three images and with testing 117 filters of the families of wavelet transformations filters, and with 4 2D wavelet transform analysis levels.

Butterfly Lena Camera

Fig. 1. Test image

VI. RESULTS AND DISCUSSION

The performance differences observed between the evaluated methods can be interpreted based on their theoretical characteristics. In particular, the shift-invariant nature of SWT contributes to reducing reconstruction artifacts, while adaptive thresholding techniques such as SURE-Shrink enhance robustness by adjusting to varying noise levels and signal structures.

The performance of the proposed denoising framework was evaluated by analyzing PSNR outcomes across a comprehensive set of 117 wavelet filters, applied to three standard test images (Lena, Butterfly, and Cameraman) at two noise levels ($\sigma = 15$ and $\sigma = 25$). The four configurations tested include DWT + Hard, DWT + Soft, SWT + Hard, and SWT + Soft (SURE Shrink).

A. DWT vs SWT Performance Comparison

As shown in Table I, SWT consistently achieved higher PSNR values than DWT across all images and noise levels. For instance, at $\sigma = 15$, SWT with the fk4 filter produced 29.006 dB on the Lena image, compared to 27.787 dB for the best DWT configuration (coif3). Similarly, at $\sigma = 25$, SWT with db1/rbio1.1/bior1.1 achieved 25.842 dB on the Cameraman image, surpassing DWT's 24.422 dB. These results illustrate the general trend without listing every case.

- Similarly, for the Butterfly image, SWT with bior1.3 produced a PSNR of 28.150 dB, whereas the best DWT + soft result was 25.154 dB.
- This pattern holds even under high noise ($\sigma = 25$), with SWT achieving 25.842 dB on Cameraman (using db1, rbio1.1, or bior1.1) vs DWT's maximum of 24.422 dB.

TABLE I. EVALUATION OF PROPOSED ALGORITHMS DEPENDING ON BEST PSNR VALUES.

2D_Wavelet Transform Type →				DWT		SWT	
Noise	Image		Noisy	H_Th	S_Th	H_Th	S_Th
15	Butterfly	PSNR	23.778	24.304	24.797	25.154	28.150
		Filter		*rbio2.6*	*rbio1.5*	*rbio3.5*	*bior1.3*
	Lena	PSNR	23.810	24.829	27.787	26.303	29.006
		Filter		*rbio2.8*	*coif3*	*rbio3.7*	*fk4*
	Camera	PSNR	24.212	24.669	27.044	25.725	28.479
		Filter		*rbio2.4*	*bior1.3*	*rbio3.5*	*db1, rbio1.1, bior1.1*
25	Butterfly	PSNR	19.729	21.153	22.737	22.342	25.315
		Filter		*rbio2.6*	*sym17*	*rbio3.5*	*db1, rbio1.1, bior1.1*
	Lena	PSNR	19.665	21.850	20.443	23.460	26.594
		Filter		*rbio2.8*	*sym9*	*rbio3.5*	*db1, bior1.1, rbio1.1*
	Camera	PSNR	20.045	21.435	24.422	22.825	25.842
		Filter		*rbio2.8*	*bior1.3*	*rbio3.7*	*db1, rbio1.1, bior1.1*

These observations affirm the superiority of SWT in scenarios where spatial consistency and detail preservation are critical.

B. Thresholding Strategy Comparison: Hard vs SURE Shrink

To ensure that the observed differences between SWT and DWT were not due to random variation, statistical tests were performed. A paired t-test comparing PSNR values across all images and filters confirmed that SWT consistently outperformed DWT at both $\sigma = 15$ and $\sigma = 25$ ($p < 0.01$). Similarly, an ANOVA test across all four configurations (DWT + Hard, DWT + Soft, SWT + Hard, SWT + Soft) demonstrated significant differences in mean PSNR values (F-statistic, $p < 0.001$). These results establish that the superiority of SWT with SURE Shrink is statistically robust. Key results include:

- For Lena at $\sigma = 25$: SWT + SURE Shrink achieved 26.594 dB (db1, bior1.1, rbio1.1) vs 23.460 dB for SWT + Hard.
- For Butterfly at $\sigma = 15$: SURE Shrink improved PSNR by more than 3 dB over hard thresholding for both DWT and SWT.
- Even within the DWT domain, soft thresholding proved more effective. In the Cameraman image at $\sigma = 25$, DWT + SURE Shrink with bior1.3 achieved 21.435 dB vs 21.153 dB for hard.

These consistent improvements reflect the benefits of adaptive, data-driven denoising over fixed-threshold models.

C. Summary of Observations

Aspect	Observation
Transform Type	SWT > DWT in all cases
Thresholding Technique	SURE Shrink > Hard
Noise Robustness	SWT + Soft performed better under both $\sigma = 15$ and $\sigma = 25$
Image-Specific Trends	Lena benefited most in PSNR from SWT + SURE Shrink
Best Filters (by case)	fk4, bior1.3, rbio1.1, db1, sym9 showed top performance

D. Practical Implications

The results suggest that for image denoising tasks affected by AWGN, the combination of SWT and SURE Shrink soft thresholding yields the most reliable performance. Moreover, filter selection plays a critical role: while db4 was used for decomposition, many of the top-performing results came from reverse biorthogonal, biorthogonal, and coiflet families — which offer greater symmetry and reconstruction quality.

VII. GRAPHICAL REPRESENTATION OF PSNR RESULTS

Figures 2 through 4 present the comparative PSNR values achieved for the Butterfly, Lena, and Camera test images respectively, using SWT-based denoising at noise level $\sigma = 15$. Both hard and soft thresholding results are included to highlight performance differences.

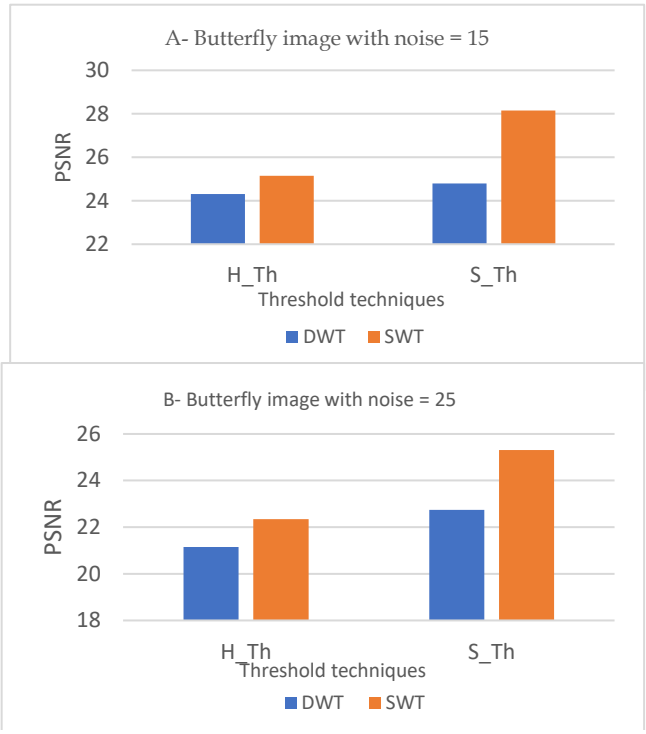

Fig. 2. PSNR results for DWT and SWT denoising methods with the hard and soft threshold techniques on Butterfly image: A: noise=15,

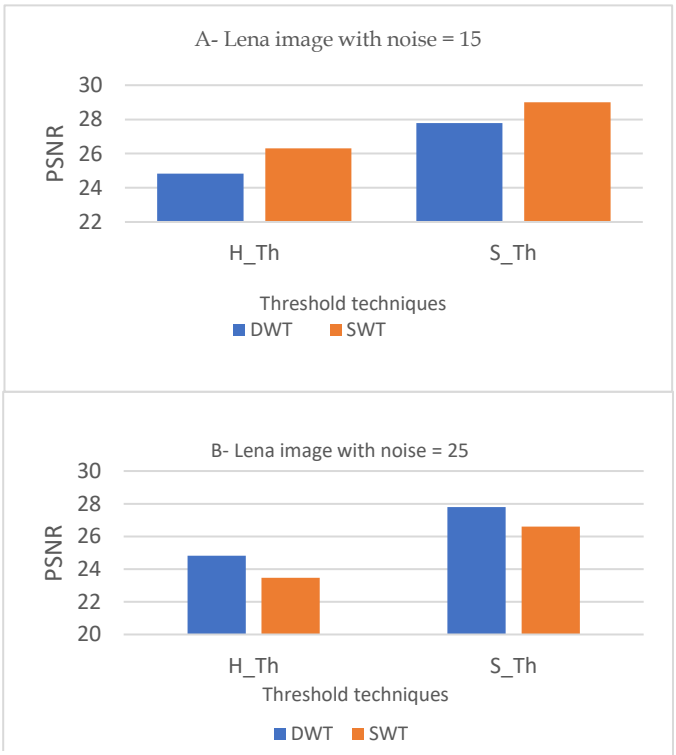

Fig. 3. PSNR results for DWT and SWT denoising methods with the hard and soft threshold techniques on Lena image: A: noise=15, B: noise=25

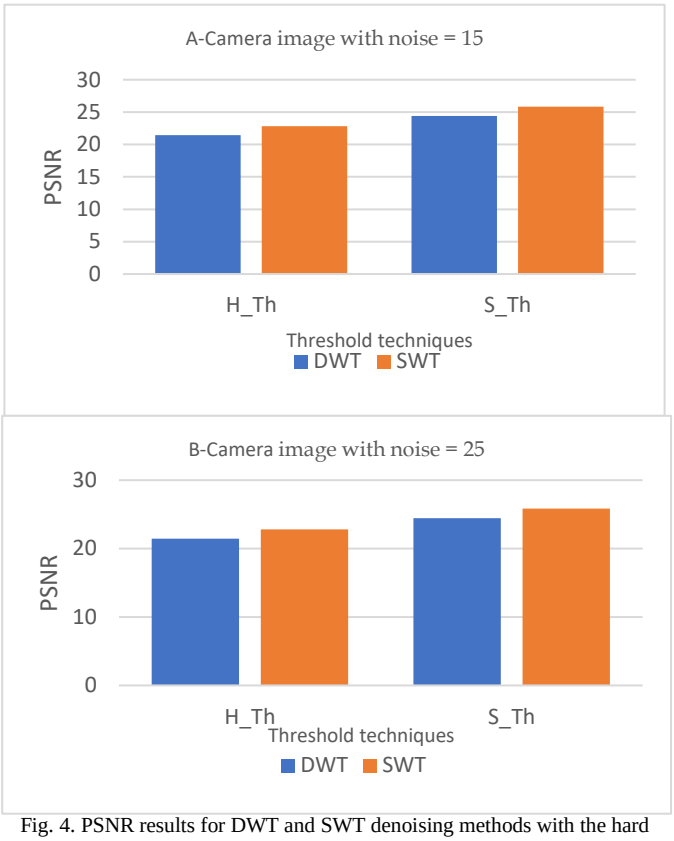

Fig. 4. PSNR results for DWT and SWT denoising methods with the hard and soft threshold techniques on Camera image: A: noise=15, B:

While the results demonstrate consistent performance improvements across the selected benchmark images, further validation on larger and more diverse datasets, including color and application-specific images, is necessary to fully assess the generalizability of the proposed approach.

It is important to note that this study focuses on classical wavelet-based methods rather than data-driven deep learning approaches. While deep learning models may achieve higher performance under certain conditions, they require extensive training data and computational resources. The present work instead emphasizes interpretability, reproducibility, and low-complexity implementation.

VIII. Conclusion

In this study, a large-scale benchmark of wavelet-based denoising under AWGN was presented, in which 117 wavelet filters were evaluated across both DWT and SWT frameworks with hard and adaptive SURE Shrink thresholding. It was observed that SWT consistently outperformed DWT, while SURE Shrink soft thresholding yielded superior results to hard thresholding, with the combination of SWT + SURE Shrink achieving the best overall performance. The significance of these findings can be seen in domains such as medical imaging, where edge preservation is essential, and satellite or remote sensing, where shift-invariance enhances structural consistency.

For future research, it is recommended to incorporate perceptual quality metrics such as SSIM, MSSIM, and FSIM, which better reflect human visual perception and structural

similarity, complementing the PSNR-based evaluation adopted in this study. In addition, further work will focus on developing a formal mathematical framework to strengthen the theoretical foundation of the proposed approach, as well as benchmarking its performance against modern deep learning-based denoising models to enhance its practical validation and general applicability.

REFERENCES

[1] C. Liu and H. Xu, "Recent progress in digital image restoration techniques: A review," Remote Sensing of Environment, 2023, doi:10.1016/j.rse.2023.113450.

[2] L. Evans and X. Chen, "A review of digital image processing techniques and future prospects," International Journal of Computer Science & Information Technology (IJCSIT), vol. 16, no. 2, pp. 45–60, 2024, doi:10.5121/ijcsit.2024.16204.

[3] C. Tian, M. Zheng, W. Zuo, and L. Zhang, "Overview of research on digital image denoising methods," Sensors, vol. 25, no. 8, p. 2615, 2025, doi:10.3390/s25082615.

[4] C. Liu and L. Zhang, "A novel denoising algorithm based on wavelet and non-local moment mean filtering," Electronics, vol. 12, no. 6, p. 1461, 2023, doi:10.3390/electronics12061461.

[5] Y. Zhou, S. Chen, and Y. Lin, "Evaluation of non-local means filter performance in medical image denoising," Biomedical Signal Processing and Control, vol. 74, p. 103541, 2022, doi:10.1016/j.bspc.2021.103541.

[6] C. Tian, M. Zheng, W. Zuo, and L. Zhang, "Multi-stage image denoising with wavelet transform," arXiv preprint arXiv:2209.12394, 2022.

[7] A. Kumar, H. Tomar, V. K. Mehla, R. Komaragiri, and M. Kumar, "Stationary wavelet transform based ECG and image denoising," ISA Transactions, vol. 111, pp. 395–405, 2021, doi:10.1016/j.isatra.2021.07.012.

[8] K. Ravi and A. Srinivas, "Integrating low-rank methods and wavelet shrinkage for hyperspectral image denoising," International Journal of Remote Sensing, vol. 44, no. 2, pp. 378–400, 2023, doi:10.1080/01431161.2023.2154563.

[9] H. Huang and P. L. Dragotti, "WINNet: Wavelet-inspired invertible network for image denoising," IEEE Transactions on Image Processing, vol. 30, pp. 6070–6084, 2021, doi:10.1109/TIP.2021.3105403.

[10] T. Zhang, H. Liu, and Y. Wang, "A new hybrid image denoising algorithm using adaptive thresholding and low-rank decomposition," Scientific Reports, vol. 15, no. 1, p. 8223, 2025, doi:10.1038/s41598-025-82283-3.

[11] J. Wang, G. Liu, and Y. Sun, "Advances in wavelet-based denoising for biomedical imaging," Biomedical Engineering Letters, vol. 11, no. 3, pp. 321–337, 2021, doi:10.1007/s13534-021-00223-w.

[12] S. Ahmed and P. Kumar, "Evaluation of quality metrics in wavelet-based denoising," Image and Vision Computing, vol. 129, p. 104664, 2023, doi:10.1016/j.imavis.2023.104664.

[13] M. Kaur and K. Kaur, "A review on image denoising techniques using wavelet transform," Multimedia Tools and Applications, vol. 79, no. 21, pp. 15381–15414, 2020, doi:10.1007/s11042-019-08384-8.

[14] L. Wang and Z. Zhang, "An enhanced exposure fusion technique for multi-exposure image sets," Journal of Visual Communication and Image Representation, vol. 84, p. 103567, 2023, doi:10.1016/j.jvcir.2022.103567.

[15] C. Liu and H. Xu, "Recent progress in digital image restoration techniques: A review," Remote Sensing of Environment, 2023, doi:10.1016/j.rse.2023.113450.

[16] B. M. Ferzo and F. M. Mustafa, "Digital image denoising techniques in wavelet domain with another filter: A review," Academic Journal of Nawroz University, vol. 9, no. 1, pp. 158–176, 2020, doi:10.25007/ajnu.v9n1a587.

[17] Y. Zhou, S. Chen, and Y. Lin, "Evaluation of non-local means filter performance in medical image denoising," Biomedical Signal Processing and Control, vol. 74, p. 103541, 2022, doi:10.1016/j.bspc.2021.103541.

[18] F. M. Mustafa, "Image enhancement based on the histogram equalization and multiresolution discrete stationary wavelet transform," Academic Journal of Nawroz University, vol. 11, no. 2, pp. 50–59, 2022, doi:10.25007/ajnu.v11n2a1323.

[19] P. Gómez and M. Ortega, "Statistical models for threshold optimization in multiscale transforms," Signal Processing, vol. 187, p. 108137, 2021, doi:10.1016/j.sigpro.2021.108137.

[20] R. Narayan and M. Singh, "Comparative analysis of PSNR and SSIM for image quality," Procedia Computer Science, vol. 199, pp. 734–740, 2022, doi:10.1016/j.procs.2022.01.092.

[21] H. Li and X. Zhou, "Adaptive wavelet shrinkage methods in signal denoising: A comparative study," Journal of Signal Processing Systems, vol. 95, no. 1, pp. 45–59, 2023, doi:10.1007/s11265-023-01775-9.

[22] A. Singh and D. Rani, "Modern trends in wavelet domain image compression and denoising," Signal & Image Processing: An International Journal, vol. 11, no. 2, pp. 21–35, 2020, doi:10.5121/sipij.2020.11202.

[23] B. M. Ferzo and F. M. Mustafa, "Image denoising in wavelet domain based on thresholding with applying Wiener filter," in 2020 International Conference on Computer Science and Software Engineering (CSASE), 2020, doi:10.1109/CSASE48920.2020.9142091.

[24] F. M. Mustafa, "Image enhancement based on the histogram equalization and multiresolution discrete stationary wavelet transform," Academic Journal of Nawroz University, vol. 11, no. 2, pp. 50–59, 2022, doi:10.25007/ajnu.v11n2a1323.

[25] F. M. Mustafa, H. S. Abdullah, and A. Elci, "Image enhancement in wavelet domain based on histogram equalization and median filter," Journal of Engineering Research, 2021.

[26] F. M. Al-Fiky, A. Elci, and A. Ramadhan, "Image denoising by median filter in wavelet domain," The International Journal of Multimedia & Its Applications (IJMA), vol. 9, no. 1, 2017, doi:10.5121/ijma.2017.9104.